J Mater Sci: Mater Med (2007) 18:2151–2157
DOI 10.1007/s10856-007-3201-8

Development of nano-sized hydroxyapatite reinforced composites for tissue engineering scaffolds

Jie Huang · Yu Wan Lin · Xiao Wei Fu · Serena M. Best · Roger A. Brooks · Neil Rushton · William Bonfield

Received: 30 March 2006 / Accepted: 1 June 2007 / Published online: 20 September 2007

Abstract Nano-sized hydroxyapatite (nanoHA) reinforced composites, mimicking natural bone, were produced. Examination by transmission electron microscopy revealed that the nanoHA particles had a rod-like morphology, 20–30 nm in width and 50–80 nm in length. The phase composition of hydroxyapatite was confirmed by X-ray diffraction. The nanoHA particles were incorporated into poly-2-hydroxyethylmethacrylate (PHEMA)/polycaprolactone (PCL) matrix to make new nanocomposites: nanoHA-PHEMA/PCL. Porous nanocomposite scaffolds were then produced using a porogen leaching method. The interconnectivity of the porous structure of the scaffolds was revealed by non-destructive X-ray microtomography. Porosity of 84% was achieved and pore sizes were approximately around 300–400 μm. An in vitro study found that the nanocomposites were bioactive as indicated by the formation of a bone-like apatite layer after immersion in simulated body fluid. Furthermore, the nanocomposites were able to support the growth and proliferation of primary human osteoblast (HOB) cells. HOB cells developed a well organized actin cytoskeletal protein on the nanocomposite surface. The results demonstrate the potential of the nanocomposite scaffolds for tissue engineering applications for bone repair.

J. Huang · Y. W. Lin · X. W. Fu · S. M. Best · W. Bonfield
Department of Materials Science and Metallurgy, University of Cambridge, Pembroke Street, Cambridge CB2 3QZ, UK

J. Huang (✉)
Department of Mechanical Engineering, University College London, Torrington Place, London WC1E 7JE, UK
e-mail: jie.huang@ucl.ac.uk

R. A. Brooks · N. Rushton
Orthopaedic Research Unit, Addenbrooke's Hospital, Box 180, Hills Road, Cambridge CB2 2QQ, UK

Introduction

A range of porous materials, such as ceramic, polymer and metal, have been developed in the field of bone grafts and scaffolds for tissue engineering [1–4]. Metals have excellent mechanical properties in terms of strength and toughness, but generally require surface modification to create favourable biological responses. Bioactive ceramics have the great advantage of encouraging bone ingrowth. But their mechanical properties, particularly the toughness is relatively poor. Polymers generally have good toughness, but their bioactivity is normally not comparable with that of bioactive ceramics. Designing a composite material to mimic the structure and properties of tissue to be replaced offers a great potential for solving these problems. Synthetic hydroxyapatite (HA) has been used extensively in biomedical implants for bone regeneration, such as coating for metallic implants, bone grafts and composites for middle ear implants [5–7]. Apatite is the major inorganic constituent in bone. The bone mineral crystals are at the nanometer scale and embedded in the collagen matrix, so bone can be considered as apatite reinforced collagen nanocomposite from a microstructural point of view. Many efforts have been made to incorporate HA into a tough polymer matrix, such as polyethylene, polylactic acid and collagen, to mimic the structure of bone [6]. However, the size of these fillers is in the micrometer range, which is at least a magnitude larger than that of the bone mineral crystals. Recent studies have shown that the incorporation of nano-sized hydroxyapatite improved the mechanical properties and protein absorption of the composite [8–9].

Nano-sized hydroxyapatite (nanoHA) particles have been produced in our laboratory [10], with sizes closer to the size of the HA crystals in natural bone. This process offers the possibility of producing new bone analogue composites by incorporating nanoHA into the polymer microstructure to further improve their mechanical and biological properties. Optimizing the structure and biological response of these nano-sized fillers is essential to the development of these nanocomposites. Our previous in vitro study showed that the nanoHA particles provided favourable anchors for primary human osteoblast-like (HOB) cell attachment, but the release of lactate dehydrogenase (LDH) was observed when human macrophages were in contact with high concentrations of the nanoHA particles, although this cytotoxicity can be diluted out [10]. In our current study, the nanoHA particles were embedded in a polymer matrix in order to minimize a potential cytotoxic effect due to the release of large quantities of nanoHA particles.

Poly-2-hydroxyethylmethacrylate (PHEMA) hydrogel is highly hydrophilic due to the presence of hydroxyl and carboxyl groups. Its non-toxicity and favourable tissue compatibility lead to a number of potential medical applications, such as drug-delivery systems and tissue engineering scaffolds [11–12]. However, the mechanical properties of PHEMA in the hydrated state are inadequate for most biomedical applications. The incorporation of linear polymer, polycaprolactone (PCL), has been made to improve mechanical performance [13–14]. The soft nature of the hydrogel, on the other hand, provides a good matrix for incorporating stiff bioactive ceramic fillers to improve the osteoconductivity of the created composite.

In this study, the nanoHA fillers were incorporated into the PHEMA/PCL system to produce new nanocomposites: nanoHA-PHEMA/PCL. Porous nanocomposite scaffolds were then made by a porogen leaching method. The structure of the nanocomposite was characterized both physically and chemically. In vitro bioactivity and biocompatibility of the nanocomposite were investigated.

Materials and methods

Production of nanoHA

NanoHA with Ca/P ratios of 1.67 was synthesised based on a precipitation reaction between calcium hydroxide ($Ca(OH)_2$) and orthophosphoric acid (H_3PO_4) (both AnalaR grade, BDH, UK). 0.3 M H_3PO_4 solution was added drop wise to 0.5 M $Ca(OH)_2$ solution under continuous stirring at room temperature, while the pH was kept above 10.5 by the addition of ammonia solution. Stirring was maintained for a further 16 h after the reactants had been added. The precipitate obtained was further aged for one week.

Characterization of nanoHA

The morphology of the nanoHA particles was examined using a JEOL 200CX transmission electron microscope (TEM) with an accelerating voltage of 200 keV. The crystal structural analysis was carried out on a Philips PW1730 X-ray diffractometer using CuK_α radiation. The data were collected from 25° to 50° with a step size of 0.05° and a scan time of 6 s.

Production of nanoHA-PHEMA/PCL composite

To produce the nanoHA-PHEMA/PCL composite, PCL (Mw = 65,000, Aldrich) pellets were melted in 2-hydroxyethyl-methacrylate (HEMA, Aldrich) at 60 °C and then mixed with 20 wt% and 40 wt% of the nanoHA fillers. Benzoyl peroxide (0.5 wt%, Fluka) was used as the initiator and ethylenglydoldimethacrylate (0.5 wt% EDGMA, Aldrich) was used as a crosslinking agent. The mixtures were then put into a mould and heated in an oven at 80 °C overnight.

The porous nanocomposite scaffold was made by the addition of 60–80 wt% of salt to the nanoHA-HEMA/PCL mixture, which was then shaped in a mould and polymerised. The salt was removed by soaking the scaffold in water for 3 days.

Characterisation of nanoHA-PHEMA/PCL composite

PHEMA is highly hydrophilic, the mass change of the nanocomposites after immersing in deionised (DI) water was monitored to measure the degree of water uptake in its hydrated state. The chemical analysis of the nanocomposites before and after immersion in DI water was performed using a Perkin-Elmer 1720-X Fourier transform infrared (FTIR) spectrophotometer. FTIR spectra were collected over the range of 4,000–600 cm^{-1}. The microstructure of hydrated nanocomposites was examined using a Philips XL 30 environmental scanning electron microscope (ESEM).

In vitro bioactivity

In addition to DI water, an acellular body fluid was used to further mimic the body environment. The simulated body fluid, SBF K9, with inorganic ion concentrations close to blood plasma was selected in this study based on the knowledge obtained from testing a wide range of materials [15]. The bioactivity of the nanocomposite was investigated by immersion in SBF K9 (pH = 7.35). The change in surface structure of the nanocomposite after soaking in SBF was studied with the use of ESEM.

Characterisation of porous nanoHA-PHEMA/PCL composite scaffold

X-ray microtomography is a non-destructive technique to provide internal and microstructural details of an object. There is no need for extensive sample preparation, and three-dimensional information can be obtained at high spatial resolution. In this study, the porosity and pore size of the scaffolds were investigated by X-ray microtomography and scanning electron microscope (SEM).

The porous scaffold samples were examined using a SkyScan-1072 high resolution desktop X-ray microtomography system (Skyscan, Belgium), which offers a maximum spatial resolution of the order of several micrometers. The X-ray radiographs were collected at 42 kv/234 μA, a 10 μm pixel size, 0.23° angle step (0°–180° rotation) and three frame averages per acquired radiograph.

A cone-beam accusation was selected and cone-beam volumetric reconstruction (Feldkamp algorithm) was employed for image reconstruction. During the image reconstruction process, the beam hardening correction papameter was set to 20–30%, depending upon the individual sample. Each original reconstructed image contained 1,024 × 1,024 pixels. The porosity and pore size were calculated and analysed using CTAn software.

The porous scaffold samples were coated with a thin layer of Pt and examined using scanning electron microscopy (JEOL 5800 SEM).

Biological response to nanoHA-PHEMA/PCL composite

A primary human osteoblast-like (HOB) cell model was used to assess the biocompatibility of each nanocomposite. The growth of HOB cells on 20 wt% and 40 wt% nanocomposite as a function of time was determined. HOB cells (2×10^4) (Promocell, GmbH) were seeded and incubated at 37 °C in a humidified air atmosphere of containing 5% CO_2. HOB cells cultured on tissue culture plastic (Tcp) were used as the test controls. The metabolic activity of HOB cells on each nanocomposite after intervals of 2, 4 and 7 days of culturing was measured using the alamarBlue™ assay (Serotec, Oxford, UK). The absorbance was measured on a plate reader at a wavelength of 570 nm with a reference wavelength of 600 nm. The absorbance with a range of cell density (1×10^4, 2×10^4, 5×10^4, 10×10^4, 20×10^4 cells/test) was measured, with the intention to correlate it with the cell number. A *t*-test was used to determine whether any significant differences existed between the mean values of absorbance measured. A difference was considered to be significant at $P < 0.05$.

Immunofluorescence

HOB cells (2×10^4 cells) (Promocell, GmbH) were seeded on the nanoHA-PHEMA/PCL composite and incubated at 37 °C in a humidified air atmosphere of 5% CO_2. The development of actin cytoskeletal proteins of the HOB cells was observed by immunofluorescence study. After 2 days in culture, the cells were fixed in 4% paraformaldehyde/PBS with 1% sucrose for 15 min. The samples were then washed with PBS and permeabilised at 4 °C for 5 min [16]. The samples were incubated with 1% bovine serum albumin (BSA)/PBS at 37 °C for 5 min to block the non-specific binding. This step was followed by the addition of FITC conjugated phalloidin (Sigma, Poole, UK) at 37 °C for 1 h. The samples were then mounted in a Vectorshield fluorescent mountant (Vector Laboratories, UK), and viewed by a Leica SP2 laser scanning confocal microscope.

Results

Characterization of nanoHA particles

TEM examination revealed that the nanoHA particles had a rod-like morphology with dimensions of 20–30 nm in width and 50–80 nm in length (Fig. 1). The selected area diffraction pattern (insert) showed the typical spotted pattern of a polycrystalline material. X-ray diffraction (XRD) patterns of the nanoHA particles indicated the presence of all the major HA peaks, such as (002), (211), (211) and (300) at 25.8°, 31.7°, 32.1°, 32.9° 2θ, as shown in Fig. 2. No secondary phases, such as tricalcium phosphate and calcium oxide, were detected.

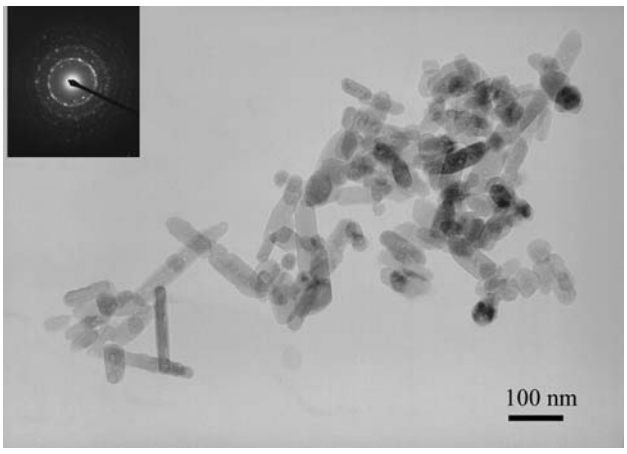

Fig. 1 TEM micrographs of the morphology of nanoHA particles. Scale bar = 100 nm. Insert is the corresponding selected area diffraction pattern

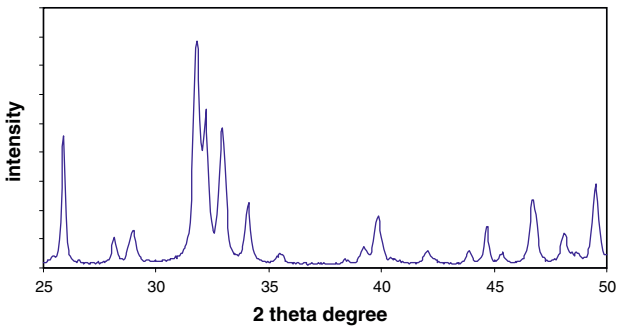

Fig. 2 X-ray diffraction patterns of nanoHA particles

Characterisation of nanoHA-PHEMA/PCL composite

The nanocomposites were hydrophilic and became rubber-like after hydration. The mass increase after 2 days immersion in DI water was 32% and 33% for the 20 wt% and 40 wt% nanoHA-PHEMA/PCL composite, respectively.

Figure 3 shows the FTIR spectrum of each nanocomposite, the peaks at 956 cm^{-1} (v_1) and 1,027 (v_3) cm^{-1} were assigned to phosphate groups of the nanoHA. The presence of HEMA was confirmed from the observed bands at 1,726 cm^{-1} (C = O stretching), 1,154 cm^{-1} (O–C–C stretching). Peaks at 1,643 cm^{-1} and 3,360 cm^{-1} corresponded to H_2O in the structure. With increasing nanoHA concentration from 20 wt% to 40 wt%, the intensity of the phosphate peak increased.

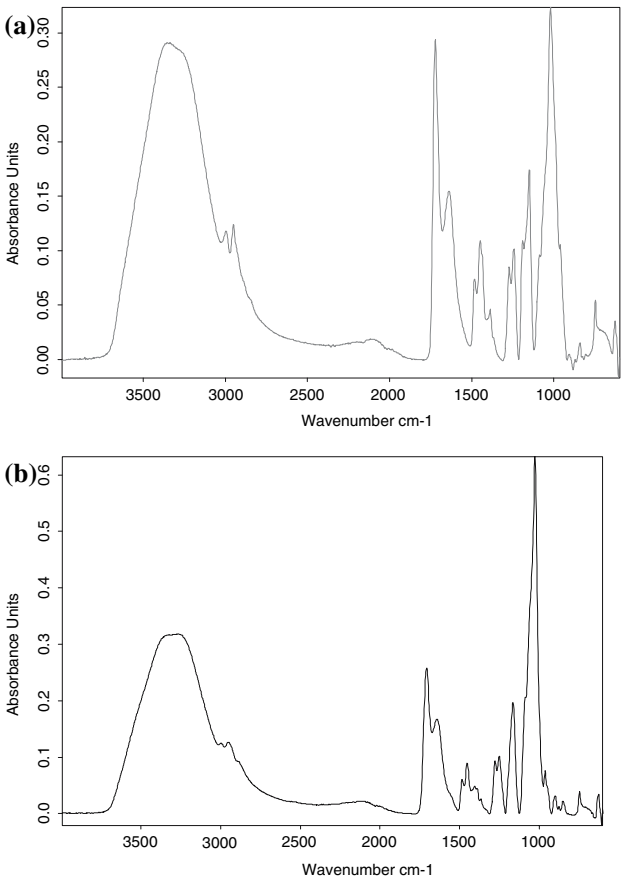

Fig. 3 FTIR spectra of 20 wt% (**a**) and 40 wt% (**b**) nanoHA-PHEMA/PCL composite after immersion in DI water

X-ray microtomography

Figure 4 shows 3-D reconstructions of the cross sections (a, b and c) of porous polymer scaffolds with porogen content from 60 wt% to 80 wt%. The interconnectivity of the pores was revealed from these scaffolds, however, the coalescence of pores was observed with a porogen content of 80 wt%. Therefore a porogen content of 70 wt% would be an optimal concentration from a structural point of view.

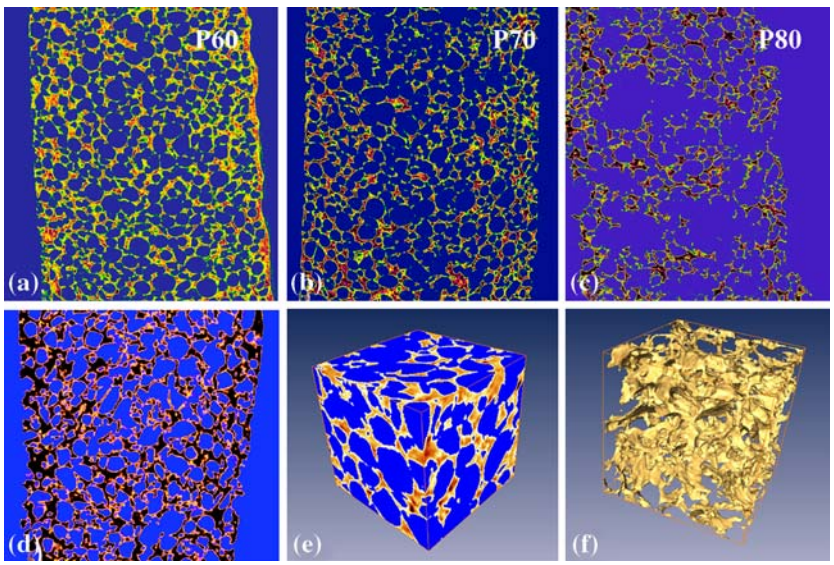

Fig. 4 Reconstruction from X-ray microtomography of porous PHEMA/PCL scaffold with porogen contents of (**a**) 60 wt%, (**b**) 70 wt% and (**c**) 80 wt%. (**d**) cross section and 3-D views of nanoHA-PHEMA/PCL scaffold with a porogen content of 70 wt% (**e** and **f**)

Table 1 The relationship between the porosity of scaffolds and porogen contents

Porogen content (wt%)	Pore volume (% of total volume) PHEMA/PCL	Pore volume (% of total volume) nanoHA-PHEMA/PCL
60	78	79
70	82	84
80	88	

The cross-section of the nanoHA-PHEMA/PCL scaffold with a porogen content of 70 wt% is shown in Fig. 4d, the interconnectivity of the pores was revealed clearly from the 3-D view (Fig. 4 e, f). The relationship between the porosity (pore volume) and porogen content is given in Table 1. With increasing porogen content, the porosity increased from 78 to 88% for PHEMA/PCL scaffolds and 79–84% for nanoHA-PHEMA/PCL scaffolds. The pore size distributions for PHEMA/PCL and nanoHA-PHEMA/PCL are shown in Fig. 5, the mean pore size was 323 and 387 μm, respectively.

Scanning electron microscopy

The microstructure of each porous scaffold was examined by SEM. Figure 6 shows both the polymer and nanocomposite scaffold contained of macropores with a size of 300 μm. The difference in the surface morphology of the nanocomposite strut was observed with the embedding of some islands of the nanoHA particles in the polymer matrix (Fig. 6d).

In vitro bioactivity

The microstructure of the hydrated nanocomposite after immersion in DI water was examined using ESEM. It was

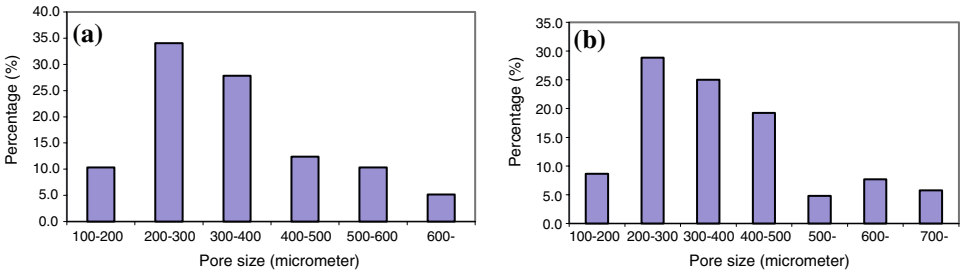

Fig. 5 The pore size distribution of (**a**) PHEMA/PCL and (**b**) 20 wt% nanoHA-PHEMA/PCL scaffolds

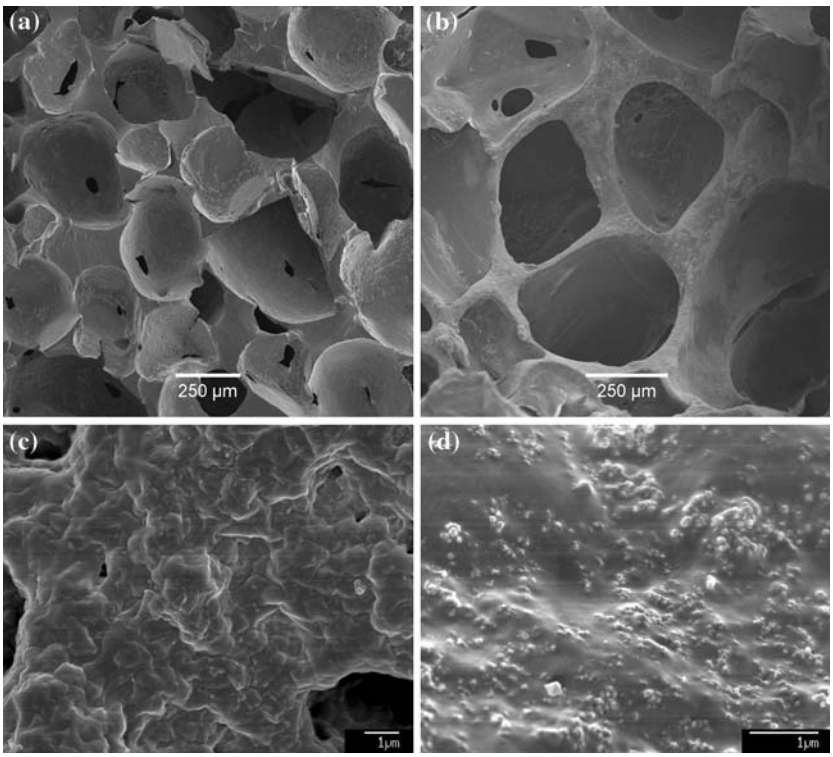

Fig. 6 SEM micrography of porous PHEMA/PCL (**a** and **c**) and 20 wt% nanoHA-PHEMA/PCL (**b** and **d**) composites, nanoHA particles embedded in the polymer matrix can be seen (**d**)

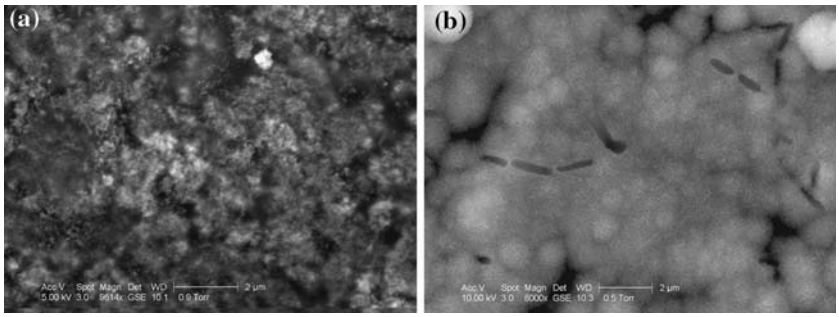

Fig. 7 ESEM micrography 40 wt% nanoHA-PHEMA composite after immersion in (**a**) DI water and (**b**) simulated body fluid, showing the formation of an apatite layer (**b**)

found that the nanoHA particles were dispersed in the polymer matrix. The difference in the surface morphology of the nanocomposite after immersion in SBF was observed. A layer of porous crystals was formed on the nanocomposite surface after 4 days immersion in SBF (Fig. 7), which was rich in calcium and phosphate from X-ray analysis, thus demonstrating the bioactivity of the nanocomposite.

Biological response of HOB cells to nanoHA-PHEMA / PCL composite

The attachment and growth of HOB cells on the 20 wt% and 40 wt% nanoHA-PHEMA/PCL composite were assessed using the alamarBlue™ assay (Serotec, Oxford, UK). All the substrates were able to support the growth of HOB cells during 7 days of culture (Fig. 8) as the absorbance increased with culture time. The calibration study found that the measured absorbance was positively correlated with cell density. Therefore, more cells were attached to the nanocomposite surface in comparison with those on the tissue culture plastic (Tcp) control at the earliest time point (2 days), which indicated that the nanocomposite provided a favourable surface for cell attachment and growth.

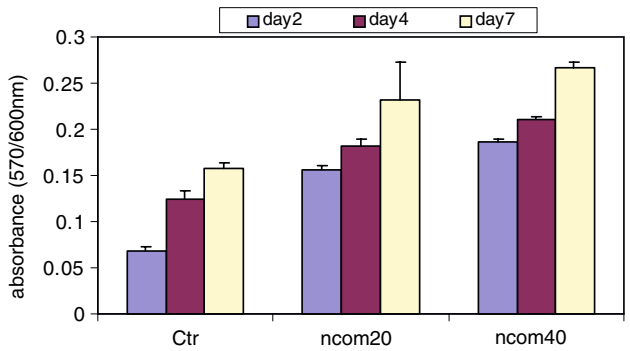

Fig. 8 Comparison of the growth of HOB cells on 20 wt% (ncom20) and 40 wt% (ncom40) nanoHA-PHEMA/PCL composites during 7 days of culture. Tissue culture plastic was used as the test control (Ctr)

HOB cells were able to spread on the nanocomposites. The development of the cell cytoskeleton of HOB cells on the nanocomposite was studied by immunofluorescent staining of actin cytoskeletal proteins. HOB cells were seen to have actin throughout their cytoskeletons after 2 days of culture. Well organised actin stress fibres of HOB cells were observed on the nanocomposites (Fig. 9).

Discussion

Apatite is the major inorganic constituent in bone, and the crystals are at nanometer scale and embedded in the collagen matrix. Although a wide range of bioactive glasses and ceramic-reinforced polymer composites have been developed to mimic bone structure, very few fillers in the nanometer range have been incorporated. In this study, nanoHA particles were produced. TEM examination

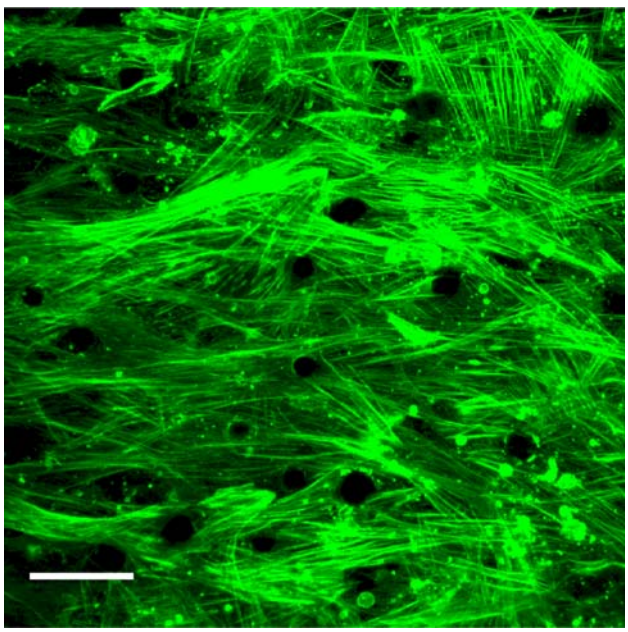

Fig. 9 Actin cytoskeletal organization (labeled with phalloidin-FITC) of HOB cells in contact with nanoHA-PHEMA/PCL composite after 2 days of culture, well organized actin stress fibres were observed. Scale bar = 40 μm

revealed that they were the rod-like with the dimensions of 20–30 nm in width and 50–80 nm in length. The spotted pattern obtained from the selected area diffraction indicated the particles were polycrystalline. The dissolution rate of crystalline HA is known to be slower than amorphous HA. The crystalline nature of these nanoHA particles was further confirmed from X-ray diffraction. Only the major HA reflection peaks, such as (002), (211), (211) and (300) were presented in the X-ray diffraction patterns of these nanoHA particles, no common secondary phases, such as tricalcium phosphate and calcium oxide were found, which confirmed the phase composition of apatite.

The cytotoxicity of nanofillers needs to be addressed carefully before designing a new nanocomposite since the release of the particulates from the matrix into the biological environment is possible. Therefore the controlled release of these nanoparticles is critical for their potential applications. In this study, the nanoHA particles were incorporated into PHEMA/PCL matrix and the potential cytotoxicity of these nanoparticles was thus inhibited. The in vitro study showed that a layer of bone-like apatite formed on the nanocomposite surface after immersion in SBF, indicating the bioactivity of the new nanocomposite. Furthermore, both 20 wt% and 40 wt% nanocomposites were able to support the growth and proliferation of HOB cells in vitro. It was found that more cells were present on the nanocomposite surface in comparison with standard tissue culture plastic control. The higher the nanoHA content, the higher the cell activity. This indicated that the nanoHA particles embedded in the polymer matrix also provided a favourable surface for HOB cell attachments, which is one of the advantages of the nanocomposites. A further study is being carried out to enhance our understanding of the new nanocomposites.

Both dense and porous nanocomposite scaffolds have been produced. It was found that the porosity of the scaffold increased with porogen content, but the coalescence of pores for the scaffold at high porogen content (80 wt%) was observed. Therefore a porogen content of 70 wt% would be optimal from a structural point of view with which an 84% porosity of the nanocomposite scaffold has been achieved.

Conclusions

NanoHA has been formulated and incorporated into the PHEMA/PCL matrix to produce both dense and porous nanocomposites. In vitro study elucidated the bioactivity and biocompatibility of these novel nanocomposites. Therefore, they are promising materials for tissue engineering applications for bone repair.

Acknowledgement Financial support from the EC for the DISC project (G5RD-CT-2000–00267) and EPSRC UK are gratefully acknowledged.

References

1. K. A. HING, S. M. BEST and W. BONFIELD, *J. Mater. Sci., Mater. Med.* **10** (1999) 135
2. H. YUAN, J. D. DE BRUIJN, X. ZHANG, C. A. VAN BLITTERSWIJK and K. DE GROOT, *J. Biomed. Mater. Res. (Appl. Biomater.)* **58** (2001) 270
3. T. M. FREYMAN, I. V. YANNAS and L. J. GIBSON, *Prog. Mater. Sci.* **46** (2001) 273
4. J. W. M VEHOF, J. MAHMOOD, H. TAKITA, M. A. VAN'T HOF, Y. KUBOKI, P. H. M SPAUWEN and J. A. JANSEN, *Plast. Reconstr. Surg.* **108** (2001) 434
5. L. L HENCH, *J. Am. Ceram. Soc*. **74** (1991) 1487
6. W. BONFIELD, M. WANG and K. E. TANNER, *Acta Materialia* **46** (1998), 2509
7. J. HUANG, L. DI SILVIO, M. WANG, K. E. TANNER and W. BONFIELD, *J. Mater. Sci., Mater. Med.* **8** (1997) 775
8. X. WANG, Y. LI, J. WEI and K. DE GROOT, *Biomaterials* **23** (2002) 4787
9. G. WEI and P. X. MA, *Biomaterials* **25** (2005) 4749
10. J. HUANG, S. M. BEST, S. N. JAYASINGHE, M. J. EDIRISINGHE, R. A. BROOKS, N. RUSHTON and W. BONFIELD, *J. Mater. Sci., Mater. Med.* **15** (2004) 441
11. L. FLYNN, P. D. DALTON and M. S. SHOICHET, *Biomaterials* **24** (2003) 4265
12. C. D. YOUNG, J. R. WU and T. L. TSOU, *Biomaterials* **19** (1998) 1745
13. L. AMBROSIO, R. DE SANTIS and L. NICOLAIS, *Proc. Inst. Mech. Eng.* **212** (1998 H) 93
14. L. AMBROSIO, P. A. NETTI, S. IANNACE, S. J. HUANG and L. NICOLAIS, *J. Mater. Sci., Mater. Med.* **7** (1996) 251
15. T. KOKUBO, H. KUSHITANI, S. SAKKA, T. KITSUGI and T. YAMAMURO, *J. Biomed. Mater. Res.* **24** (1990) 721
16. M. J. DALBY, L. DISILVIO, E. J. HARPER and W. BONFIELD, *Biomaterials* **23** (2002) 569